

# Anomalous Motion of Particle Levitated by Laguerre-Gaussian beam

Yang Li,<sup>1</sup> Lei-Ming Zhou,<sup>1,2</sup> and Nan Zhao<sup>1,\*</sup>

<sup>1</sup>*Quantum Physics and Quantum Information Division,  
Beijing Computational Science Research Center, Beijing 100193, China*

<sup>2</sup>*Department of Electrical and Computer Engineering,  
National University of Singapore, Singapore 117583, Singapore*

Laguerre-Gaussian (LG) beam has orbital angular momentum (OAM). A particle trapped in an LG beam will rotate about the beam axis, due to the transfer of OAM. The rotation of the particle is usually in the same direction as that of the beam OAM. However, we discover that when the LG beam is strongly focused, the rotation of the particle and the beam OAM might be in the opposite direction. This anomalous effect is caused by the negative torque on the particle exerted by the focused LG beam, which is similar to the optical pulling force in the linear case. We calculated the scattering force distribution of a micro-particle trapped in an optical tweezers formed by the strongly focused LG beam, and showed that there exist stable trajectories of the particle that controlled by the negative torque. We proposed several necessary conditions for observing the counter-intuitive trajectories. Our work reveals that the strongly trapped micro-particle exhibits diversity of motion patterns.

## I. INTRODUCTION

Optical tweezers use radiation force of laser beams to trap or manipulate micro- or nano-particles. Since the first discovery of laser trapping of particles [3, 4, 8], optical tweezers techniques have attracted more and more interest in the fundamental research and applications, ranging from molecular biology to high-precision measurement [11, 19]. Optical tweezers have become an important tool for studying the non-equilibrium process of deoxyribonucleic acid (DNA) in molecular biology [5, 15, 17, 20]. Recently, optical tweezers were also used to study the basic problems of thermodynamics and to develop new types of quantum devices [12, 16, 18, 28].

The fundamental Gaussian mode of laser beams are the common choice for the optical tweezers experiments [9, 27, 29]. In recent years, laser beams with various non-trivial modes, such as Bessel beams and Laguerre-Gaussian (LG) beams [2, 10, 13, 19, 21, 30], were introduced in the optical tweezers systems. Among those laser beams, the LG beams, which carry orbit angular momentum (OAM) and exert torque to the trapped particles [1, 26, 30, 31], can be used to manipulate the angular motion of the particles. Meanwhile, with the angular motion considered, the particle exhibits remarkable differences in trapping stability [22, 23]. Environmental dissipation (friction) is essential to stabilize the angular motion of the particle.

In an optical tweezers system, the beams of non-trivial spatial modes lead to many counter intuitive phenomena, such as the backward pulling force generated by a forward propagating Bessel beam [6, 7, 14, 24, 25]. Moreover, the strongly focused laser beams exhibit different physical characteristics from the paraxial beams. In the paraxial beam case, an  $LG_{pl}$  beam carries well-defined OAM with

the quantum number  $l$ . A particle trapped in the paraxial LG beam would feel a torque in the same direction of OAM. However, when the LG beam is strongly focused, the field distribution of the beam is significantly modified. We found that the torque exerted on the particle is unnecessarily the same as the OAM of the trapping beam. In the following, we refer to the torque opposite to the OAM as the optical negative torque (ONT).

The ONT will significantly affect the angular motion of the trapped particles. Driven by the ONT, the particle can rotate in the opposite direction to the OAM of the trapping LG beam. A key question is whether the anomalous trajectories is stable, so that they could be observed experimentally. We used Lorentz-Mie theory to calculate force field of the particle in the strongly focused laser beam and studied the motion of the particle in the different dissipative environments. We found that the dissipation caused by the residual pressure is crucial to the trapping stability and the anomaly of motion. With suitable dissipation, the anomalous trajectory of the particle driven by the ONT would form a stable circle orbit. Besides, the orbits is robust against to the perturbations on position and velocity of the particle. We systematically study the dependence of the ONT on the laser intensity, particle size and environmental dissipation, and propose a feasible manipulation project in experiment.

## II. FORCE AND MOTION

We consider a micro-particle which is trapped by strongly focused Laguerre-Gaussian beams. Figure 1(a) shows the electric field distribution of a typical circularly polarized  $LG_{pl}$  beam with wavelength  $\lambda = 1064 \mu\text{m}$  and the radial index  $p = 0$  and azimuth index  $l = 3$ . Because of the non-zero OAM, the intensity distribution on the beam focal plane exhibits a bright ring. Small particles with  $R \ll \lambda$  are usually trapped on the bright ring, which corresponding to a double-well “optical potential” in the

\* nzhao@csrc.ac.cn

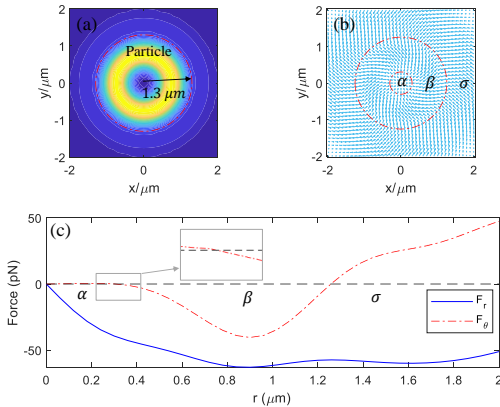


Figure 1. (a) The intensity distribution of a strongly focused  $LG_{03}$  beam in the focal plane. (b) The distribution of the radiation force exerted on a particle of radius  $R = 1.3 \mu\text{m}$ . (c) The radial and azimuthal components of the radiation force, as functions of the center-of-mass radius of the trapped particle. According to the sign of the azimuthal force  $F_\theta$ , the focal plane can be divided into three regions. In the second region  $\beta$ , the direction of the optical torque is opposite to the direction of the OAM of the beam.

radial direction. However, for large particles with  $R \sim \lambda$  in our case, the center of the trapped particle coincides the dark point of the beam [31].

Figure 1(b) shows the radiation force exerting on the center of mass (CoM) of a glass spherical particle with refraction index  $n = 1.5$  and radius  $R = 1.3 \mu\text{m}$ . The force field  $F(r_{CoM})$  in the circularly polarized LG beam is rotational invariant. Figure 1(c) shows the radial component and azimuthal component,  $F_r$  and  $F_\theta$ , respectively. The radial force is always negative ( $F_r < 0$ ) which indicates that the optical force tends to pull the particle to the beam center. However, the azimuthal component changes sign as increasing the radial distance  $r_{cm}$  of the trapped particle. There are three regions, according to the sign of the azimuthal force [see Figs. 1(b)&(c)]. Particularly, the azimuthal force become negative in the region with  $0.3 \mu\text{m} < r < 1.2 \mu\text{m}$ . The optical torque  $\tau$  exerted on the particle is in the same direction of the OAM of the  $LG_{03}$  beam in the regions  $\alpha$  and  $\sigma$ , while in the region  $\beta$  the particle feels an ONT.

The counter-intuitive ONT causes non-trivial motion of the trapped particle. We consider the equations of motion of the particle,

$$\begin{aligned} m\ddot{r} - mr\dot{\theta}^2 &= F_r - \gamma(P)\dot{r}, \\ 2m\dot{r}\dot{\theta} + mr\ddot{\theta} &= F_\theta - \gamma(P)\dot{\theta}, \end{aligned} \quad (1)$$

where  $m$  is the mass of the particle,  $\gamma(P)$  is the friction coefficient due to the residual gas. The transient motion relies on the initial conditions of the particle (e.g., initial position and velocity), which are usually not well-controlled. Here, we focus on the stable rotation of the particle, which can be conveniently observed in experiments. Due to the rotational symmetry of the radiation

force, an obvious solution of Eq. (1) is a uniform circular motion with  $\dot{r} = 0$  and  $\dot{\theta} = 0$ . In this case, the radial force  $F_r$  provides the centripetal force, and the azimuthal force  $F_\theta$  is compensated by the friction force.

For a given pressure  $P$ , the two requirements in Eqs. (1)&(1) determine the possible radius  $R^*$  of the circle orbit. In the low damping limit, Eqs. (1)&(1) have no solution, which means the friction is too weak to slow down the angular motion of the particle. While in the high damping limit, Eqs. (1)&(1) only have trivial solution of  $R^* = 0$ . The particle, in this case, is confined around the beam center. In the intermediate region, as shown in Fig. 2(a), there exists several non-trivial solutions that the particle can have stable circular orbits. More interestingly, some of the orbits lie in the ONT region, where the angular velocity is opposite to the OAM of the trapping beam. We refer to the counter-intuitive motion driven by the ONT of the strongly focused LG beams as the anomalous motion of the particle in the following.

To be observed in real experiments, the anomalous motion should be robust against to perturbation. To analyze the robustness of the anomalous motion, we expand Eq. (1) around the circle solution. With  $r(t) = r_0 + \delta r(t)$  and  $\theta(t) = \theta_0 + \delta\theta(t)$  and keeping up to the linear terms of the fluctuations  $\delta r(t)$  and  $\delta\theta(t)$ . Using the normalization factor  $\frac{1}{\gamma r_0}$ , the Equation (1) is linearized as

$$\begin{pmatrix} \dot{a} \\ \dot{b} \\ \dot{c} \end{pmatrix} = \begin{pmatrix} 0 & \frac{\gamma}{m} & 0 \\ \frac{m\omega^2 + k_1}{\gamma} & -\frac{\gamma}{m} & 2\omega \\ \frac{k_2 - \gamma\omega}{\gamma} & -2\omega & -\frac{\gamma}{m} \end{pmatrix} \begin{pmatrix} a \\ b \\ c \end{pmatrix} \quad (2)$$

with setting  $a = \frac{1}{r_0}\delta r$ ,  $b = \frac{m}{\gamma r_0}\delta\dot{r}$  and  $c = \frac{m}{\gamma}\delta\dot{\theta}$ , where  $\partial_r F_r = \partial F_r / \partial r|_{r=r_0}$  and  $\partial_r F_\theta = \partial F_\theta / \partial r|_{r=r_0}$  are the derivatives of the radiation force components with respect to the orbits radius. The eigenvalues  $\{\lambda_i\}_{i=1}^3$  of the coefficient matrix determine the stability of the circle orbits. A robust orbit requires that the real part of the eigenvalues should be negative, i.e.,  $Re[\lambda_i] < 0$  for  $i = 1, 2$  and  $3$ . Figure (2)b shows the maximal value of the real part of three eigenvalues, i.e.,  $A_{max} = \max_i[Re[\lambda_i]]$ , as a function of the circular orbit radius. The particle can have robust circle orbits with both positive and negative angular velocity.

The dependence of radius of the robust circle orbits on the pressure exhibits non-trivial behavior. In generic cases (e.g., trapping with Gaussian mode beams), the radius of the circle orbit would be decreased if one increases the environmental dissipation by increasing the pressure. However, the inset of Fig. 2 shows an anomalous expansion of the orbit size as increasing pressure. This is essentially caused by the non-trivial angular force distribution of the strongly focused LG beam (see Fig. 1).

Figure 3 shows the typical trajectories of the trapped particle in different regions under small perturbation. Given an environmental pressure, e.g.,  $P = P_D$ , the cor-

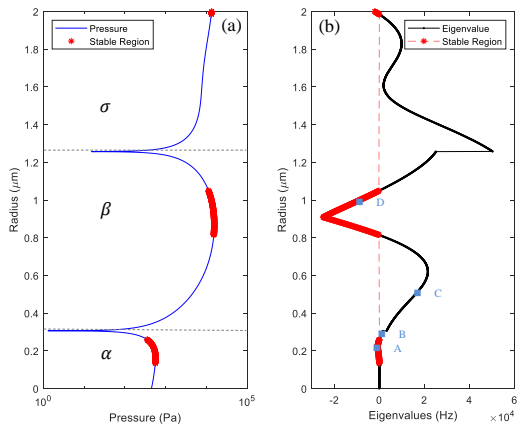


Figure 2. (a) The circle orbits radius as a function of the given environmental pressure  $P$ . Three regions are in the same as the regions defined in Fig. (1). (b) The eigenvalue  $\Lambda_{max}$  in the perturbation analysis. The orbits with  $\Lambda_{max} < 0$  is stable (indicated by red symbols). Four representative orbits are denoted by A - D, which are clockwise stable orbit, clockwise unstable orbit, counter-clockwise unstable orbit, and counter-clockwise stable orbit, respectively.

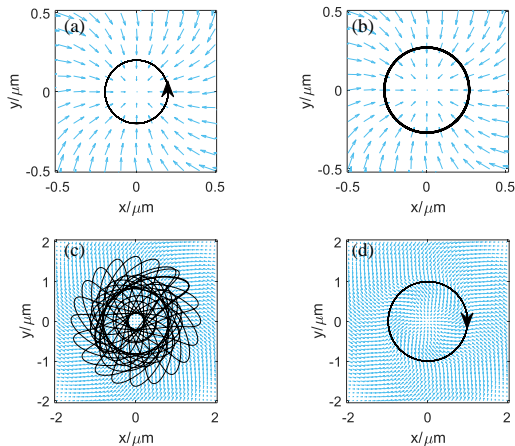


Figure 3. The representative trajectories corresponding to the points A - D in Fig. 2 under small perturbations. (a) The stable orbit corresponding to point A. The angular velocity of the particle is the same as the OAM of the beam. (b) & (c) The unstable orbit corresponding to points B and C. The radius of the particle oscillates in the trap. (d) The stable orbit corresponding to point D. The angular velocity of the particle is opposite to the OAM of the beam.

responding steady-state radius and angular velocity of the circular motion is  $r = r_D$  and  $\dot{\theta} = \sqrt{F_r(r_D)/mr_D}$ , where  $P_D$  and  $r_D$  are the coordinates of the point  $D$  denoted in Fig. 2. Figure 3(a) shows the transient trajectory with the initial radius perturbed by an amount of 1%, i.e.,  $\delta r/r_A = 0.01$ . Since the point A is in the stable region, the initial perturbation decays with time, and the particle is stabilized at the orbit with radius  $r = r_A$ . The

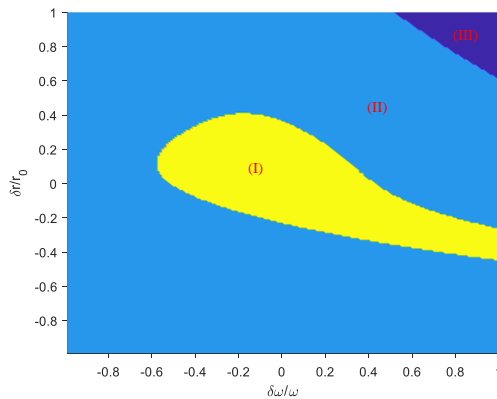


Figure 4. Robustness of the anomalous motion under strong disturbance. The horizontal axis is the relative change of the initial radius to the radius  $r_D$  in Fig. 3(d). The vertical axis is the relative change of the initial angular velocity to the angular velocity  $\theta_D$  in Fig. 3(d). In the yellow region (I), the particle is stabilized at the anomalous orbit ( $r = r_D$ ). In the blue region (II), the particle is end up at the beam axis ( $r = 0$ ). In the purple region (III), the disturbance is so strong that the particle escapes from the trap.

angular momentum is in the same direction of the OAM of the trapping beam (counter-clockwise). However the same amount perturbation around the unstable trajectories (e.g., the point B and point C in Fig. 2) causes complex motions of the particle. For small perturbation ( $\delta r/r_B = \delta r/r_C = 0.01$ ), the radius  $r(t)$  oscillates around the steady-state solutions  $r_B$  and  $r_C$  [as shown in Figs. 3(b) and 3(c)], while strong perturbation may cause the particle escape from the trap. Similar to Fig. 3(a), Fig. 3(d) shows the stable trajectory in the anomalous region around the point D in Fig. 2. Driven by the ONT, the particle has opposite angular momentum direction (clockwise) to the OAM.

To further study the robustness of the anomalous motion in Fig. 3(d), we calculate the particle's trajectory under strong disturbance. We consider the initial radius and the initial angular velocity deviations in a region of  $\delta r/r_D = [-1, 1]$  and  $\delta \theta/\theta_D = [-1, 1]$ . With different initial disturbance, the particle will end up with three states in long term: (i) the stable anomalous orbit ( $r = r_D$ ); (ii) the beam axis ( $r = 0$ ); and (iii) escaping from the optical trap ( $r = \infty$ ). Figure 4 shows that the particle can suffer quite strong disturbance [as strong as  $\sim 40\%$  in both initial radius and initial angular velocity, see the yellow region (I)]. This result indicates that the anomalous motion is robust, and is possible to be observed even with not very precise control of the particle.

### III. CONCLUSION

In summary, we have studied the motion of a particle trapped in a strongly focused LG beam. We predict that, similar to the optical pulling force in the linear cases, the

strongly focused beam can provide counter-intuitive optical torques, i.e., the optical negative torques. We further show that, the optical negative torques can drive the trapped particle rotating in the opposite direction of the OAM of the trapping LG beam. With the analysis of the motion stability, we conclude that the anomalous motion driven by the ONT can be observed in experiments.

This work is supported by NKBPR (973 Program) 2016YFA0301201, the Science Challenge Project (Grant No. TZ2018003), NSFC No. 11534002 and NSAF U1930402. L.-M. Z. acknowledges the support from Ministry of Education, Singapore (Grant No. R-263-000-D11-114).

- 
- [1] L. Allen, M. W. Beijersbergen, R. J. C. Spreeuw, and J. P. Woerdman. Orbital angular momentum of light and the transformation of laguerre-gaussian laser modes. *Physical Review A*, 45(11):8185–8189, jun 1992. doi:10.1103/physreva.45.8185.
- [2] J Arlt, V Garces-Chavez, W Sibbett, and K Dholakia. Optical micromanipulation using a bessel light beam. *Optics Communications*, 197(4-6):239–245, oct 2001. doi:10.1016/s0030-4018(01)01479-1.
- [3] A. Ashkin. Acceleration and trapping of particles by radiation pressure. *Physical Review Letters*, 24(4):156–159, jan 1970. doi:10.1103/physrevlett.24.156.
- [4] A. Ashkin, J. M. Dziedzic, J. E. Bjorkholm, and Steven Chu. Observation of a single-beam gradient force optical trap for dielectric particles. *Optics Letters*, 11(5):288, may 1986. doi:10.1364/ol.11.000288.
- [5] Steven M. Block, David F. Blair, and Howard C. Berg. Compliance of bacterial flagella measured with optical tweezers. *Nature*, 338(6215):514–518, apr 1989. doi:10.1038/338514a0.
- [6] Jun Chen, Jack Ng, Zhifang Lin, and C. T. Chan. Optical pulling force. *Nature Photonics*, 5(9):531–534, jul 2011. doi:10.1038/nphoton.2011.153.
- [7] Jun Chen, Jack Ng, Kun Ding, Kin Hung Fung, Zhifang Lin, and C. T. Chan. Negative optical torque. *Scientific Reports*, 4(1), sep 2014. doi:10.1038/srep06386.
- [8] Steven Chu. Laser trapping of neutral particles. *Scientific American*, 266(2):70–76, feb 1992. doi:10.1038/scientificamerican0292-70.
- [9] Maria Dienerowitz. Optical manipulation of nanoparticles: a review. *Journal of Nanophotonics*, 2(1):021875, sep 2008. doi:10.1117/1.2992045.
- [10] S. Franke-Arnold, L. Allen, and M. Padgett. Advances in optical angular momentum. *Laser & Photonics Review*, 2(4):299–313, aug 2008. doi:10.1002/lpor.200810007.
- [11] Dongliang Gao, Weiqiang Ding, Manuel Nieto-Vesperinas, Xumin Ding, Mahdy Rahman, Tianhang Zhang, ChweeTeck Lim, and Cheng-Wei Qiu. Optical manipulation from the microscale to the nanoscale: fundamentals, advances and prospects. *Light: Science & Applications*, 6(9):e17039, mar 2017. doi:10.1038/lsa.2017.39.
- [12] Jan Gieseler, Romain Quidant, Christoph Dellago, and Lukas Novotny. Dynamic relaxation of a levitated nanoparticle from a non-equilibrium steady state. *Nature Nanotechnology*, 9(5):358–364, mar 2014. doi:10.1038/nnano.2014.40.
- [13] Lei Gong, Weiwei Liu, Qian Zhao, Yuxuan Ren, Xingze Qiu, Mincheng Zhong, and Yinmei Li. Controllable light capsules employing modified bessel-gauss beams. *Scientific Reports*, 6(1), jul 2016. doi:10.1038/srep29001.
- [14] Veerachart Kajorndejnkul, Weiqiang Ding, Sergey Sukhov, Cheng-Wei Qiu, and Aristide Dogariu. Linear momentum increase and negative optical forces at dielectric interface. *Nature Photonics*, 7(10):787–790, aug 2013. doi:10.1038/nphoton.2013.192.
- [15] Wojciech K. Kasprzak, Taejin Kim, My-Tra Le, Feng Gao, Megan Y.L. Young, Xuefeng Yuan, Joonil Seog, Anne E. Simon, and Bruce A. Shapiro. Simulations of optical tweezers experiments reveal details of RNA structure unfolding. *Biophysical Journal*, 114(3):214a–215a, feb 2018. doi:10.1016/j.bpj.2017.11.1199.
- [16] May E. Kim, Tzu-Han Chang, Brian M. Fields, Cheng-An Chen, and Chen-Lung Hung. Trapping single atoms on a nanophotonic circuit with configurable tweezer lattices. *Nature Communications*, 10(1), apr 2019. doi:10.1038/s41467-019-09635-7.
- [17] Scot C. Kuo and Michael P. Sheetz. Optical tweezers in cell biology. *Trends in Cell Biology*, 2(4):116–118, apr 1992. doi:10.1016/0962-8924(92)90016-g.
- [18] Tongcang Li, Zhe-Xuan Gong, Zhang-Qi Yin, H. T. Quan, Xiaobo Yin, Peng Zhang, L.-M. Duan, and Xiang Zhang. Space-time crystals of trapped ions. *Physical Review Letters*, 109(16), oct 2012. doi:10.1103/physrevlett.109.163001.
- [19] Onofrio M. Maragò, Philip H. Jones, Pietro G. Gucciardi, Giovanni Volpe, and Andrea C. Ferrari. Optical trapping and manipulation of nanostructures. *Nature Nanotechnology*, 8(11):807–819, nov 2013. doi:10.1038/nnano.2013.208.
- [20] J. Millen, T. Deesuwan, P. Barker, and J. Anders. Nanoscale temperature measurements using non-equilibrium brownian dynamics of a levitated nanosphere. *Nature Nanotechnology*, 9(6):425–429, may 2014. doi:10.1038/nnano.2014.82.
- [21] T S Monteiro, J Millen, G A T Pender, Florian Marquardt, D Chang, and P F Barker. Dynamics of levitated nanospheres: towards the strong coupling regime. *New Journal of Physics*, 15(1):015001, jan 2013. doi:10.1088/1367-2630/15/1/015001.
- [22] Jack Ng, Z. F. Lin, C. T. Chan, and Ping Sheng. Photonic clusters formed by dielectric microspheres: Numerical simulations. *Physical Review B*, 72(8), aug 2005. doi:10.1103/physrevb.72.085130.
- [23] Jack Ng, Zhifang Lin, and C. T. Chan. Theory of optical trapping by an optical vortex beam. *Physical Review Letters*, 104(10), mar 2010. doi:10.1103/physrevlett.104.103601.
- [24] Jack Ng, Jun Chen, Zhifang Lin, and C. T. Chan. Pulling particles backward using a forward propagating beam. *The Journal of the Acoustical Society of America*, 131(4):3533–3533, apr 2012. doi:10.1121/1.4709367.
- [25] Andrey Novitsky, Cheng-Wei Qiu, and Haifeng Wang. Single gradientless light beam drags particles as tractor

- beams. *Physical Review Letters*, 107(20), nov 2011. doi: 10.1103/physrevlett.107.203601.
- [26] N. B. Simpson, K. Dholakia, L. Allen, and M. J. Padgett. Mechanical equivalence of spin and orbital angular momentum of light: an optical spanner. *Optics Letters*, 22(1):52, jan 1997. doi:10.1364/ol.22.000052.
- [27] Bidisha Sinha, Darius KÅ¶ster, Richard Ruez, Pauline Gonnord, Michele Bastiani, Daniel Abankwa, Radu V. Stan, Gillian Butler-Browne, Benoit Vedic, Ludger Johannes, Nobuhiro Morone, Robert G. Parton, Graça Raposo, Pierre Sens, Christophe Lamaze, and Pierre Nassoy. Cells respond to mechanical stress by rapid disassembly of caveolae. *Cell*, 144(3):402–413, feb 2011. doi: 10.1016/j.cell.2010.12.031.
- [28] Pimonpan Sompert, Stuart S. Szigeti, Eyal Schwartz, Ashton S. Bradley, and Mikkel F. Andersen. Thermally robust spin correlations between two 85rb atoms in an optical microtrap. *Nature Communications*, 10(1), apr 2019. doi:10.1038/s41467-019-09420-6.
- [29] W. H. Wright, G. J. Sonek, and M. W. Berns. Radiation trapping forces on microspheres with optical tweezers. *Applied Physics Letters*, 63(6):715–717, aug 1993. doi: 10.1063/1.109937.
- [30] ZHANG-QI YIN, ANDREW A. GERACI, and TONG-CANG LI. OPTOMECHANICS OF LEVITATED DIELECTRIC PARTICLES. *International Journal of Modern Physics B*, 27(26):1330018, oct 2013. doi: 10.1142/s0217979213300181.
- [31] Lei-Ming Zhou, Ke-Wen Xiao, Jun Chen, and Nan Zhao. Optical levitation of nanodiamonds by doughnut beams in vacuum. *Laser & Photonics Reviews*, 11(2):1600284, mar 2017. doi:10.1002/lpor.201600284.